Mesoscopic and Microscopic Modeling of Island Formation in Strained Film Epitaxy

Zhi-Feng Huang
Department of Physics and Astronomy, Wayne State University, Detroit, Michigan 48201, USA

K. R. Elder
Department of Physics, Oakland University, Rochester, Michigan 48309, USA

(Received 23 June 2008; published 7 October 2008)

The instability of strained films for island formation is examined through an approach incorporating both discrete microscopic details and continuum mechanics. A linear relationship between the island wave number and misfit strain is found for large strains, while only in the small strain limit is a crossover to the continuum elasticity result obtained. A universal scaling relation accommodating all range of misfit strains is identified. Our results indicate that continuum mechanics may break down even at relatively small misfit stress due to the discrete nature of crystalline surfaces.

DOI: 10.1103/PhysRevLett.101.158701 PACS numbers: 68.55.−a, 81.15.Aa, 89.75.Da, 89.75.Kd

Strained film epitaxy has become one of the most important techniques in the manufacturing and processing of nanoscale materials. While growth conditions for epitaxial films are often chosen to suppress stress-induced instabilities, in many cases these instabilities can be exploited for the self-assembly of interesting nanostructures such as quantum dots and nanowires on predefined substrates [1]. Understanding the fundamental mechanisms responsible for film growth and evolution is thus essential for both suppression and exploitation of these instabilities, as encountered in a broad variety of physical systems that are dependent on epitaxial films. Most exploitation efforts have focused on the growth of coherent, defect-free structures, and on the control of long-range ordering and size or shape regularity as desired in optoelectronic device applications. For the example of coherent quantum dots or strained islands [1–3], the formation of such surface nanostructures is expected from a stress-driven, morphological instability of the Asaro-Tiller-Grinfeld (ATG) type [4–6]. Subsequent evolution involves island shape transition [7,8] and dynamic coarsening [8–10], as observed in recent experiments on, e.g., Ge/Si and SiGe/Si. For large enough islands, further stress release will lead to the nucleation of misfit dislocations [11].

Despite such complexities much progress has been made in the modeling of the self-assembly process. Continuum elasticity theory has provided insight into the initial morphological instability [5,6,12,13], island shape evolution [8,14], and coarsening [15–18]. Such an approach is well suited for the long-wavelength behavior of the system, but does not incorporate the influence of the film crystalline structure. Details of the crystalline structure can be captured via atomistic modeling such as kinetic Monte Carlo simulations (with the incorporation of elastic energy [19,20]), but these models are typically (computationally) limited to small scales.

The focus of this Letter is on an approach that naturally incorporates the discrete nature of a crystalline lattice and standard continuum theory on large scales, which can be applied to a wider range of applications that involve elasticity at the nano and meso scales. More specifically, this work is based on the phase field crystal (PFC) model which models the "*small*" length scale of crystalline structures on *diffusive* time scales [21,22]. To extend the applicability of this model to larger scales, we analyze the amplitudes or envelopes of the *slowly varying* film surface profile. This multiscale treatment leads to a crossover behavior of film properties at different misfits, showing the importance of the film crystalline nature.

Here, we consider island formation on strained epitaxial films. Classic continuum theory predicts that at the early stages of growth, the island periodicity (λ_I) is inversely proportional to the misfit strain (ε_m) squared [5,6] (similar result is obtained even when wetting effects are included [14,18]). However, this result disagrees with experiments on SiGe/Si(001) [2,3] showing $\lambda_I \propto \varepsilon_m^{-1}$. Current theory to account for this discrepancy is based on the surface diffusivity difference between film components [12,17], a feature that is specific for alloys and verified recently by first-principle calculations [23]. Our study here suggests that such ε_m^{-1} scaling is more general, and a crossover to the continuum ATG result occurs only in the small misfit, long-wavelength limit. Such qualitatively different behavior is related to an upper limit on island wave number imposed by the condition of "perfect" lattice relaxation as will be discussed latter.

To illustrate the phenomena of interest, typical simulation results are shown in Fig. 1 for two (2D) and three (3D) dimensional island formation in semi-infinite strained films. In this limit, a unique solution can be obtained for λ_I, and it is sufficient to introduce strain in the initial condition only, given an initial constrained film with the lattice constant different from its equilibrium bulk state. The simulations are based on the PFC model in which the free energy functional $\mathcal{F}$ can be derived from classical density functional theory and expressed in terms of a

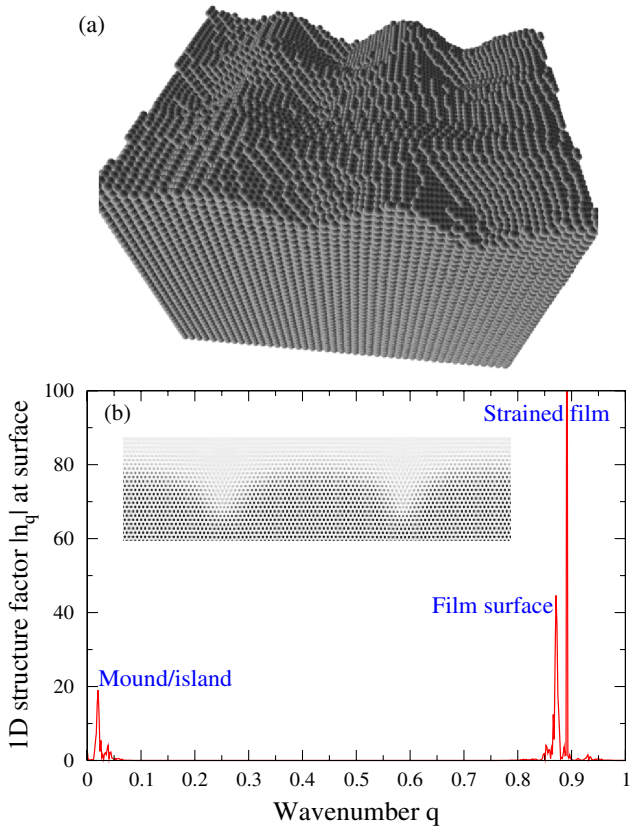

FIG. 1 (color online). (a) Gray scale image of epitaxial islands in 3D PFC simulations, for a 4.8% tensile film of 512^3 grid size at $t = 31200$ and with $B^l = 1$ and $B^s = 0.988$. (b) The 1D structure factor along the film surface for a 2D 2.9% compressive film with grid size 4096×2048, $B^l = 9.8$, and $B^s = 10$.

rescaled atomic density field $n(\boldsymbol{r}, t)$ [22]:

$$\Delta\mathcal{F}/\bar{\rho}k_BT = \int d\boldsymbol{r}[B^s n(R^2\nabla^2 + 1)^2 n/2 + (B^l - B^s)n^2/2 - n^3/6 + n^4/12 - \cdots], \quad (1)$$

where $\Delta\mathcal{F} = \mathcal{F} - \mathcal{F}(n = 0)$, $\bar{\rho}$ is the average atomic density, T is the temperature, and R is proportional to the lattice spacing. This model yields a liquid-solid transition controlled by $\epsilon = (B^s - B^l)/B^s$ (>0 for solid phase) which can be related to temperature difference from the melting point. The solid phase has hexagonal or triangular symmetry in 2D and bcc in 3D, and this model naturally incorporates elasticity, plastic deformations, crystalline anisotropy, anisotropic surface energy [24], and anisotropic and temperature dependent elastic constants $C_{11}/3 = C_{12} = C_{44} \propto B^s$ [21]. The dynamics of n is assumed to be conserved, dissipative, and driven to minimize $\mathcal{F}$, i.e., $\partial n/\partial t = \Gamma\nabla^2\delta\mathcal{F}/\delta n + \eta$, where η is due to the thermal noise and Γ sets the time scale for dynamic processes. After rescaling (with a length scale $l_0 = R$ and time scale $\tau_0 = R^2/\Gamma B^s$), we have

$$\partial n/\partial t = \nabla^2[-\epsilon n + (\nabla^2 + q_0^2)^2 n - gn^2 + n^3] + \eta, \quad (2)$$

where $g = (3/B^s)^{1/2}/2$ and $q_0 = 1$.

Details of both microscopic structure and larger-scale morphological profile can be captured by Eq. (2) (see Fig. 1), as well as the basic sequence of strained film evolution observed in experiments (instabilities $\rightarrow$ islands $\rightarrow$ dislocations [21,22]). Quantitative results have been obtained, with an example shown in Fig. 1(b) for the 1D power spectrum at film surface. The three peaks in this figure, from right to left, correspond to the original strained lattice, the relaxed surface lattice, and the larger-scale profile of surface islands. The island peak shifts to smaller wave number at later times and finally disappears when misfit dislocations nucleate and reduce the misfit stress responsible for the initial instability.

While direct simulation of Eq. (2) is useful, it is difficult to access the large time and length scales relevant for small misfit strains. To access such scales, we extend the amplitude expansion approach for the PFC model as put forth by Goldenfeld *et al.* [25], particularly to incorporate a slow-scale ($\mathcal{O}(\epsilon^{1/2})$) average density field n_0 which is needed to describe liquid-solid coexistence and a miscibility gap [26]. We follow the standard multiple scales approach [27] that separates "slow" scales for the evolution of surface profiles and "fast" scales of the underlying crystalline structure. For 2D films, in the limit of small ϵ, the density field can be described as a superposition of 3 base modes of the hexagonal structure, with the associated *complex* amplitudes varying on slow scales $(X, Y, T) = (\epsilon^{1/2}x, \epsilon^{1/2}y, \epsilon t)$, i.e., $n = n_0(X, Y, T) + \sum_{j=1}^{3} A_j(X, Y, T)e^{i\boldsymbol{q}_j^0\cdot\boldsymbol{r}}$ + c.c. (with $\boldsymbol{q}_j^0$ the three hexagonal basic wave vectors). This yields

$$\partial A_j/\partial t = -q_0^2\delta\mathcal{F}/\delta A_j^*, \quad \partial n_0/\partial t = \nabla^2\delta\mathcal{F}/\delta n_0, \quad (3)$$

$$\begin{aligned}\mathcal{F} = \int d\boldsymbol{r}\Big\{&(-\epsilon + 3n_0^2 - 2gn_0)\sum_{j=1}^{3}|A_j|^2 \\ &+ \sum_{j=1}^{3}|(\nabla^2 + 2i\boldsymbol{q}_j^0\cdot\boldsymbol{\nabla})A_j|^2 \\ &+ \frac{3}{2}\sum_{j=1}^{3}|A_j|^4 + (6n_0 - 2g)(A_1A_2A_3 + A_1^*A_2^*A_3^*) \\ &+ 6(|A_1|^2|A_2|^2 + |A_1|^2|A_3|^2 + |A_2|^2|A_3|^2) - \frac{1}{2}\epsilon n_0^2 \\ &+ \frac{1}{2}[(\nabla^2 + q_0^2)n_0]^2 - \frac{1}{3}gn_0^3 + \frac{1}{4}n_0^4\Big\}. \end{aligned} \quad (4)$$

A linear stability analysis of these equations can now be conducted to examine the instability of strained films to buckle and form mounds/islands. This will be accomplished by linearizing around a planar interface separating a liquid and strained film.

For a strained film with misfit ε_m, the hexagonal lattice is distorted, and the amplitudes can be expressed by $A_{1,3} = A'_{1,3}e^{i(\mp\delta_x x - \delta_y y/2)}$ and $A_2 = A'_2e^{i\delta_y y}$, where $\delta_x = \sqrt{3}q_0\varepsilon_m/2$ and δ_y is determined by lattice relaxation along

the y direction (perpendicular to the film surface) [28]. For a base state involving a planar surface along the x direction, the amplitudes A_j^0 and n_0^0 only depend on the normal direction y and are also governed by Eqs. (3) and (4) (with $\partial_x = 0$). We have calculated the equilibrium profile for this 1D base state, corresponding to nongrowing planar films with liquid-solid coexistence. We find that larger B^s (proportional to bulk modulus) leads to more diffuse liquid-solid interface, and also to smaller miscibility gap which slightly decreases with misfit ε_m.

Except for zero misfit, such 1D base-state profiles are unstable against surface/interface perturbations due to strain energy relaxation. This is examined by expanding

$$A_j'(x, y, t) = A_j^0(y) + \sum_{q_x} \hat{A}_j(q_x, y, t) e^{iq_x x}, \tag{5}$$

$$n_0(x, y, t) = n_0^0(y) + \sum_{q_x} \hat{n}_0(q_x, y, t) e^{iq_x x}. \tag{6}$$

The time evolution of the perturbed quantities $\hat{A}_j$ and $\hat{n}_0$ is derived by substituting Eqs. (5) and (6) into (3), and retaining up to 1st order of $\hat{A}_j$ and $\hat{n}_0$. The resulting coupled equations with spatially dependent coefficients can now be solved numerically.

The results are summarized in Figs. 2 and 3. For strained films, there exists a range of wave number q_x within which initial small random perturbations of $\hat{A}_j$ and $\hat{n}_0$ grow exponential in time near the film/liquid surface and decay to zero in the solid and liquid bulk regions. A typical example is shown in the inset of Fig. 2. To obtain an estimate of the island size, we assume that the Fourier amplitude with largest growth rate (maximally unstable) determines the characteristic island wave number Q_I ($=2\pi/\lambda_I$). This wave number is shown in Fig. 2 as a function of misfit strain for several values of B^s (which controls the magnitude of the elastic constants). This plot reveals two distinct regimes. For small values of ε_m, we obtain $Q_I \sim \varepsilon_m^2$, while for large values, $Q_I \sim \varepsilon_m$.

The small ε_m result is consistent with continuum elasticity theory (i.e., an ATG instability [5,6,14,18]). More precisely, the ATG instability predicts that the most unstable wave vector Q_I is proportional to $(E/\gamma)\varepsilon_m^2$, where E and γ are Young's modulus and the surface tension, respectively. The constant of proportionality depends on the precise mechanism (i.e., evaporation/condensation, surface diffusion, or bulk diffusion) which is difficult to decouple in this model and may also be influenced by the nature of the liquid-solid interface. To evaluate this prediction, we have calculated Young's modulus E analytically in a one-mode approximation and the surface tension γ numerically as a function of strain and B^s. For small ε_m, all the data fit the relationship $Q_I = (4/3)(E/\gamma)\varepsilon_m^2$ very well (see inset of Fig. 3).

For large ε_m, it is useful to consider the upper limit on Q_I imposed by the discrete nature of the lattice. For the simple 2D hexagonal lattice considered here, the film can completely relieve the strain by nucleating dislocations at an appropriate distance (λ_R) apart. This distance can be determined as follows. Let the number of atoms in strained surface lattice be N (before dislocation nucleation), and the number of atoms unstrained (after dislocations nucleate) be M. By definition, the length (L) of the film must obey $L = Na = Ma_0$, where a is the lattice constant of strained film and a_0 is the unstrained, bulk lattice constant. Thus, the misfit strain is $\varepsilon_m = (a_0 - a)/a = (N - M)/M$, and the average distance between dislocations $\lambda_R = L/|N - M| = a_0/\varepsilon_m$. It is unphysical for the system to produce islands that are smaller than the wavelength λ_R needed for "perfect" relaxation (although continuum theory does make this prediction). A line representing this upper limit is shown in Fig. 2 (i.e., $Q_I = Q_o\varepsilon_m$, with $Q_o = 2\pi/a_0$).

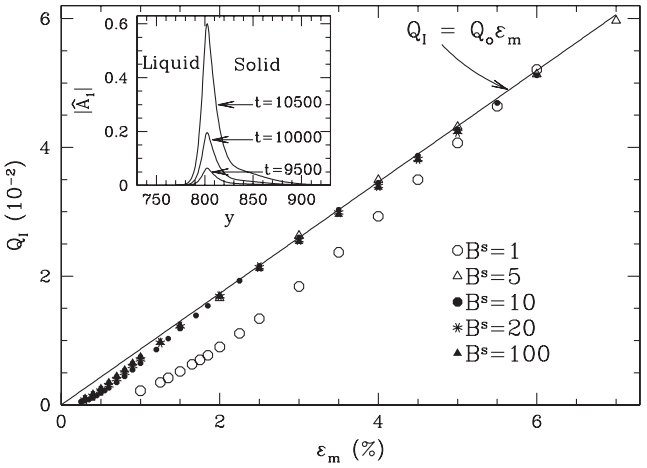

FIG. 2. Characteristic wave number Q_I as a function of misfit ε_m, for $L_y = 4096$, $\epsilon = 0.02$, and various values of B^s. The solid line corresponds to "perfect" relaxation as discussed in the text. In the inset, the growth of amplitude perturbation is shown for $B^s = 1.0$, $\varepsilon_m = 7\%$, and $Q_I = 0.055$ as a function of y (the direction perpendicular to the surface).

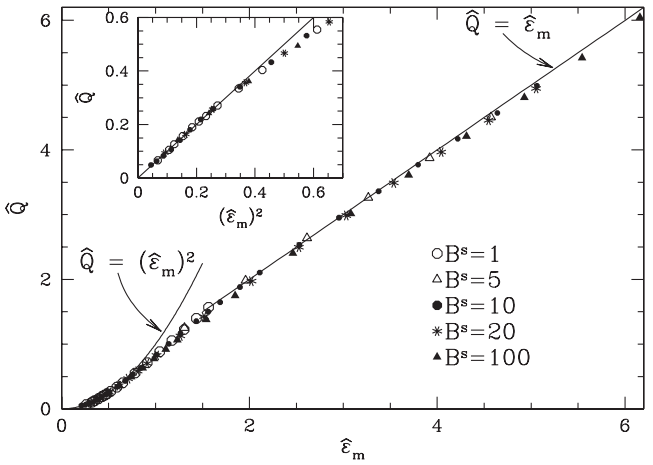

FIG. 3. Scaling of island wave vector as a function of misfit strain; see text for definition of scaled variables. In the inset, the ATG region at small misfits is expanded.

As can be seen in this figure, the numerical results converge to this line in the large ε_m limit. For more complex 3D multicomponent systems, λ_R will depend on the details of the dislocation nucleation pathways which may involve some intermediate partially relaxed states or be influenced by compositional inhomogeneities.

The results presented in Fig. 2 can be scaled onto a single universal curve by assuming that Q_I is described by the ATG instability in the small ε_m limit and by ''perfect'' relaxation in the large ε_m limit. The crossover of the two limits occurs when $(4E/3\gamma)\epsilon_m^2 = Q_o\epsilon_m$, yielding a crossover misfit strain and island wave vector of $\epsilon_m^* = 3\gamma Q_o/4E$ and $Q_I^* = 3\gamma Q_o^2/4E$. If both Q_I and ϵ_m are scaled at this point, i.e., $\hat{Q} \equiv Q_I/Q_I^*$ and $\hat{\epsilon}_m \equiv \epsilon_m/\epsilon_m^*$, the data can be reduced to the scaling curve shown in Fig. 3. The data convergence to this universal curve works well for all range of misfits and different values of B^s (related to materials of different elastic constants), even for very small $\hat{\epsilon}_m$ as shown in the inset. Since the arguments presented above do not depend on the sign of the misfit strain, the scaling results should be valid for both compressive and tensile strains. However, this is not to imply that Q_I and the crossover parameters (Q_I^* and ϵ_m^*) are the same since film properties (e.g., surface tension γ, liquid-solid interface width, etc.) are very likely to depend on the sign of the strain.

These scaling results indicate that for pure film systems, the essential parameter responsible for wavelength selection and crossover behavior is γ/E, not γ (surface tension) or E (Young's modulus) separately, a factor that would be valuable for the important issue of quantum dot or island size control. In addition, the crossover behavior of island size scaling indicates a more complicated role of misfit strain on quantum dot evolution, and the identification of crossover parameters (ϵ_m^* and Q_I^*) should provide a new avenue in characterizing nanostructure (islands/dots) formation and properties.

In summary, we have developed an approach that incorporates continuum elasticity and crystalline symmetry and gives insight into the mechanisms of strained film instability and island formation. Based on PFC modeling and particularly on the analysis of amplitude equations governing the slowly varying surface profile, we obtain a linear regime for the island wave number scaling and recover the continuum ATG instability in the weak strain limit. All ranges of data are found to obey a universal scaling relation that characterizes the crossover from the ATG limit to the ''perfect'' lattice relaxation condition. These results also emphasize the importance of the crystalline nature of strained films, which in this work is incorporated by phase perturbations of the complex, mesoscopic-scale amplitudes (A_j). These amplitudes naturally incorporate nonlinear relaxation processes that are absent in continuum elasticity theory. Finally, we note that while a linear relationship between island wave number and misfit strain has been observed in some experiments (i.e., SiGe/Si(001)), these experiments contain additional factors (such as differing atomic mobilities of film components) that may account for such behavior. For this reason, it would be interesting to experimentally examine this phenomena in pure systems to directly test the predictions of this work.

We are indebted to Kuo-An Wu and Peter Voorhees for helpful discussions. K. R. E. acknowledges the support from NSF under Grant No. DMR-0413062.

[1] J. Stangl, V. Holy, and G. Bauer, Rev. Mod. Phys. **76**, 725 (2004).
[2] P. Sutter and M. G. Lagally, Phys. Rev. Lett. **84**, 4637 (2000).
[3] R. M. Tromp, F. M. Ross, and M. C. Reuter, Phys. Rev. Lett. **84**, 4641 (2000).
[4] R. J. Asaro and W. A. Tiller, Metall. Trans. **3**, 1789 (1972); M. A. Grinfeld, Sov. Phys. Dokl. **31**, 831 (1986).
[5] D. J. Srolovitz, Acta Metall. **37**, 621 (1989).
[6] B. J. Spencer, P. W. Voorhees, and S. H. Davis, Phys. Rev. Lett. **67**, 3696 (1991).
[7] J. Tersoff *et al.*, Phys. Rev. Lett. **89**, 196104 (2002).
[8] A. Rastelli *et al.*, Phys. Rev. Lett. **95**, 026103 (2005).
[9] F. M. Ross, J. Tersoff, and R. M. Tromp, Phys. Rev. Lett. **80**, 984 (1998).
[10] J. A. Floro *et al.*, Phys. Rev. Lett. **84**, 701 (2000).
[11] D. E. Jesson *et al.*, Science **268**, 1161 (1995).
[12] B. J. Spencer, P. W. Voorhees, and J. Tersoff, Phys. Rev. B **64**, 235318 (2001); J. Tersoff, Phys. Rev. Lett. **85**, 2843 (2000).
[13] Z.-F. Huang and R. C. Desai, Phys. Rev. B **65**, 205419 (2002); Phys. Rev. B **65**, 195421 (2002).
[14] B. J. Spencer and M. Blanariu, Phys. Rev. Lett. **95**, 206101 (2005).
[15] F. Liu, A. H. Li, and M. G. Lagally, Phys. Rev. Lett. **87**, 126103 (2001).
[16] K. Kassner *et al.*, Phys. Rev. E **63**, 036117 (2001).
[17] Y. Tu and J. Tersoff, Phys. Rev. Lett. **98**, 096103 (2007).
[18] M. S. Levine *et al.*, Phys. Rev. B **75**, 205312 (2007).
[19] M. T. Lung, C. H. Lam, and L. M. Sander, Phys. Rev. Lett. **95**, 086102 (2005).
[20] G. Nandipati and J. G. Amar, Phys. Rev. B **73**, 045409 (2006).
[21] K. R. Elder *et al.*, Phys. Rev. Lett. **88**, 245701 (2002); Phys. Rev. E **70**, 051605 (2004).
[22] K. R. Elder *et al.*, Phys. Rev. B **75**, 064107 (2007).
[23] L. Huang *et al.*, Phys. Rev. Lett. **96**, 016103 (2006).
[24] K. A. Wu *et al.*, Phys. Rev. B **73**, 094101 (2006).
[25] N. Goldenfeld, B. P. Athreya, and J. A. Dantzig, Phys. Rev. E **72**, 020601(R) (2005); B. P. Athreya, N. Goldenfeld, and J. A. Dantzig, Phys. Rev. E **74**, 011601 (2006).
[26] D. H. Yeon, Z.-F. Huang, K. R. Elder, and K. Thornton (unpublished).
[27] M. C. Cross and P. C. Hohenberg, Rev. Mod. Phys. **65**, 851 (1993).
[28] For the amplitude equations to be valid, A_j should be slowly varying and hence δ_x, δ_y, ε_m be sufficiently small.